Multi-Messenger Coincident Search

A Joint Detection of Gravitational-Waves, High-Energy Neutrinos and Gamma-Ray Bursts

Internship Report for PHY592

Xitian Huang

September 2023

Contents

1 Introduction **1**
1.1 Multi-Messenger Astronomy 1
1.2 LLAMA 1
1.3 HPMOC 4
1.4 Aim 6

2 Theoretical Model **6**
2.1 Hypothesis Counting 6
2.1.1 Stirling and Bell numbers 7
2.2 Hypothesis Testing 7

3 Implementation **10**
3.1 A Background Cascade Simulation 10
3.2 GW-Neutrino-GRB Significance Calculation 12
3.3 GRB data 15

4 Conclusion **17**

A Appendix **22**

1 Introduction

Ever since ancient times, humans have been observing the sky with naked eyes and different cultures have, in one way or another, attributed various different meanings to astronomical phenomena. Technology then gave birth to many tools used for astronomical observation, from the classical optical telescope to telescopes in invisible regime such as radio and infrared. They are also subdivided by the astronomical phenomena. For instance, the Fermi Gamma-ray Space Telescope, which is a satellite orbiting the Earth since 2008, and more recently the IceCube detector in south pole dedicated to detecting neutrinos, and LIGO, a high precision laser interferometer devoted to gravitational-wave detection. These are only a few typical examples. In fact, there're innumerable other detectors and telescopes working around the clock both on the ground and orbiting the Earth, collecting tremendous amount of data every second. When such big amount of data is concerned, a proper data analysis technique is crucial to locate the information that is important to us. Fortunately, each detector has its own team working on analysing the data. But difficulty arises when one tries to combine data from different detectors to extract more useful information. This is where multi-messenger astronomy comes into play.

1.1 Multi-Messenger Astronomy

Astronomical events are violent and usually they emit several signals in a short period of time. It is therefore natural to consider all the different signals, i.e., messengers, together. This deepens our understanding of the particular event. Two notable examples are first observed supernova SN1987A [4] where both gamma-rays and neutrinos were detected, and gravitational-waves GW170817 [2] where a subsequent gamma-ray burst (GRB) follow-up was detected. A manual operation of finding such coincidental events from different detectors would be very tedious. The GCN (General Coordinates Network) helps to solve this. It is a real-time collaborative platform by NASA to share alerts and communications from all different detectors on transient phenomena and trigged events.

1.2 LLAMA

One of the many software used in multi-messenger astronomy is LLAMA [8] (Low-Latency Algorithm for Multi-messenger Astrophysics). The current version of LLAMA provides a fast algorithm that checks whether the incoming data of neutrinos and gravitational-waves are significant, i.e., it infers how likely a particular neutrino and a particular GW may come from the same source. It contains a pipeline for the whole process of accepting the data, extracting the information, calculating the significance and push the calculation to the team in real time. Figure 1 illustrates this.

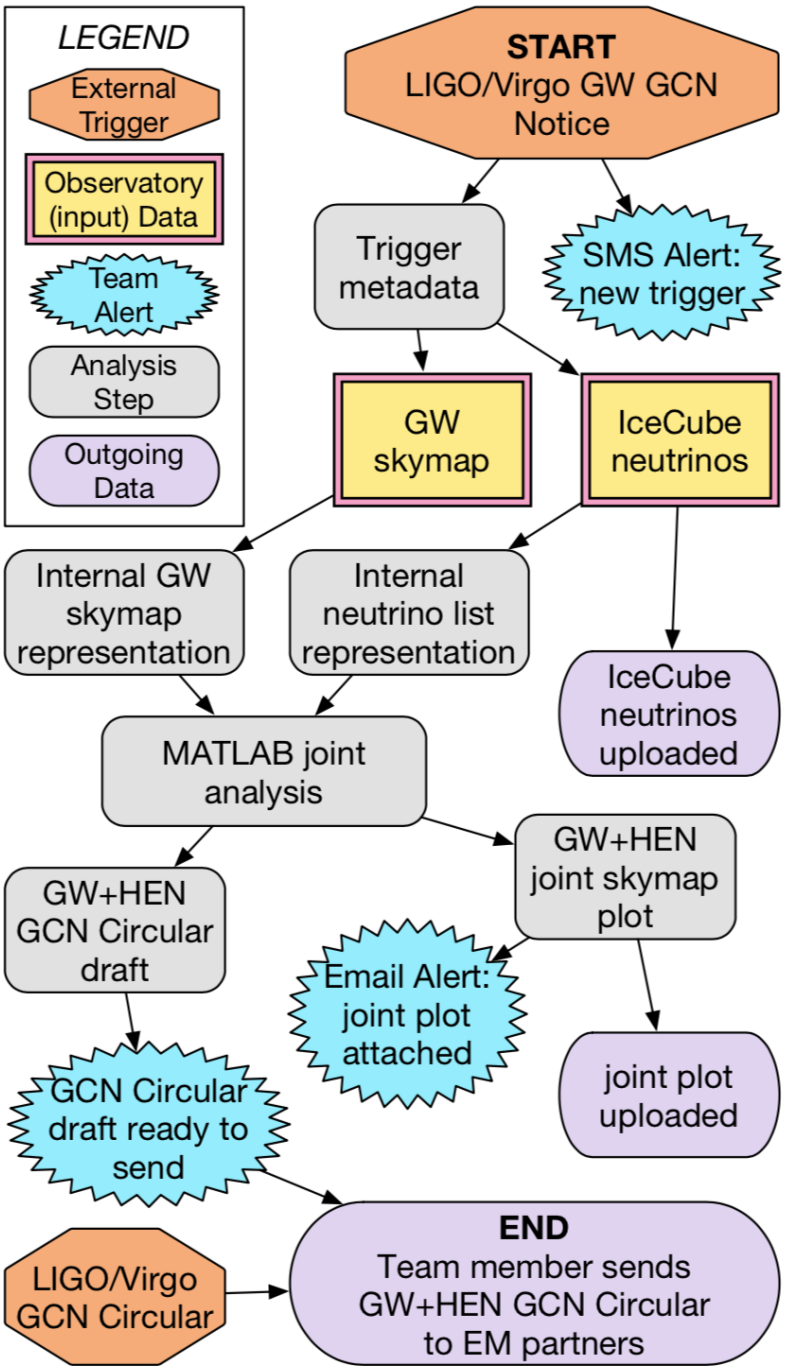

Figure 1: Diagram that shows the structure of LLAMA, the flow of the data and the operations performed in each step.

Specifically, the data inside LLAMA has a hierarchical structure. Figure 2 shows how all the incoming data files depends on one another. LVC stands for LIGO-VIRGO Collaboration. I3 is short for IceCube and *OPA* for Open Public Alert. It's only a label of events saying that the event is a confirmed event. The opposite of OPA would be *subthreshold*, indicating that the detected signal might be noise.

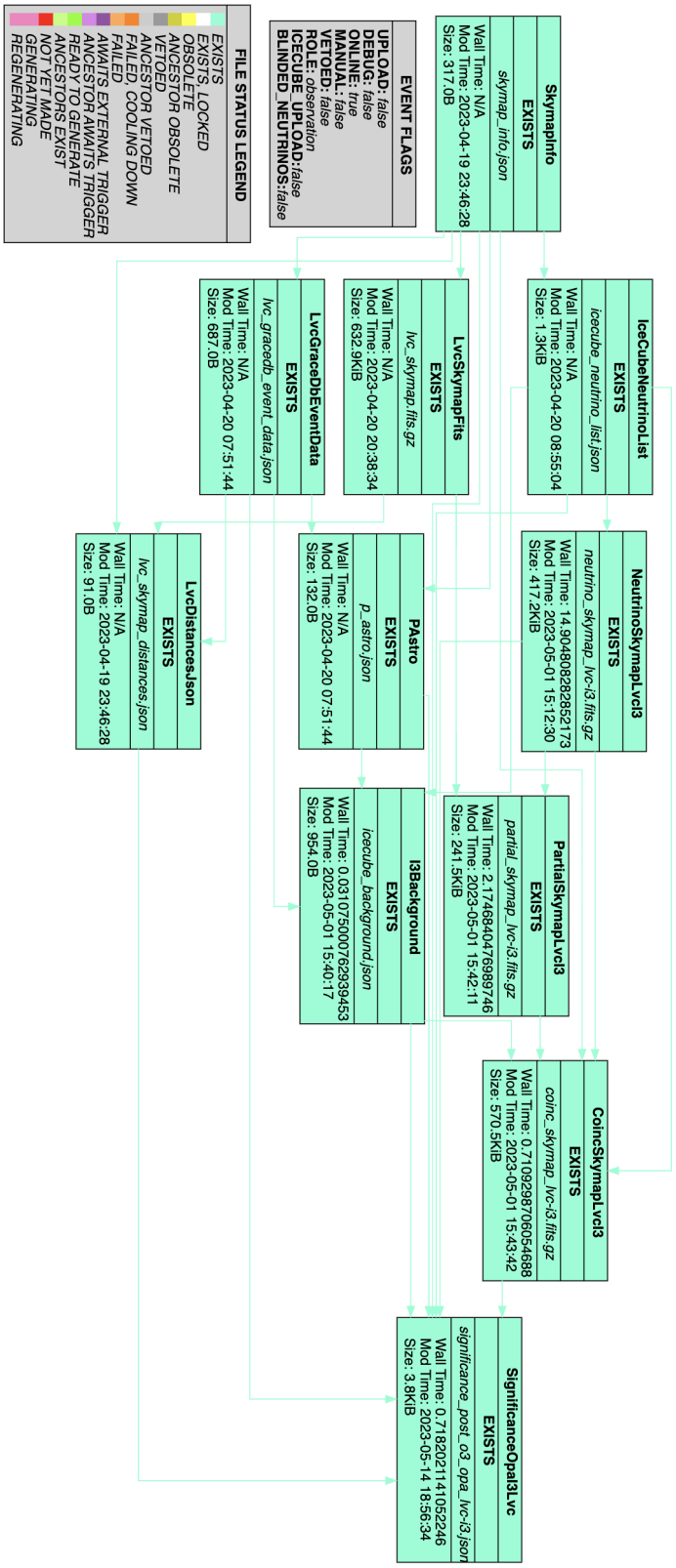

Figure 2: LLAMA in OPA mode. Files on the right have dependencies on files on the left.

The core part of LLAMA is its calculation of significance between events. Figure 3 shows how the

odds ratio in the end is calculated based on the input data. A higher odds ratio indicates a higher chance that the events may be of the same astronomical event. The algorithm of the calculation follows a Bayesian inference. [6]

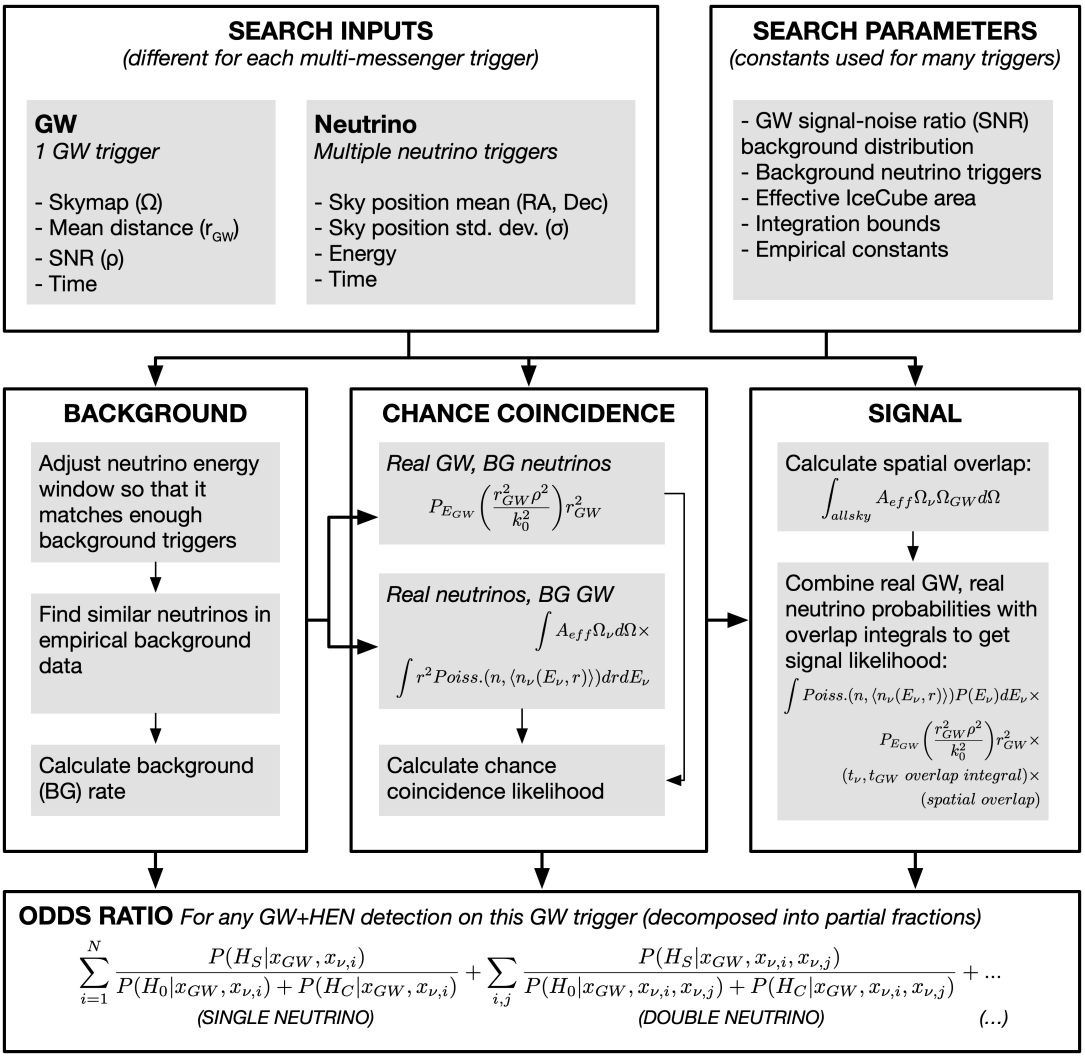

Figure 3: Flowing chart showing the significance calculation of LLAMA.

1.3 HPMOC

Detectors used in astrophysics are running all day long and the data it captured has to been store in a way that is easy to access, efficient to manipulate and small in size. The data are usually in the form of *skymap* (as `fits` (Flexible Image Transport System) file [11]), namely, a spherical map on which every point has some particular information such as the probability density. A framework known as HEALPix [9] (Hierarchical Equal Area iso-Latitude Pixelization), widely used in observational astronomy nowadays, is used to store data captured from detectors. It divides the sphere into discrete pixels with equal area. The centres of each pixel are aligned on the same altitude for different altitudes. Pixels can be subdivided, to increase the precision of the skymap if necessary. The reverse of subdivision then decreases the precision. Figure 4 shows how it works. HEALPix also has other features such as indexing and support for fast harmonic transform.

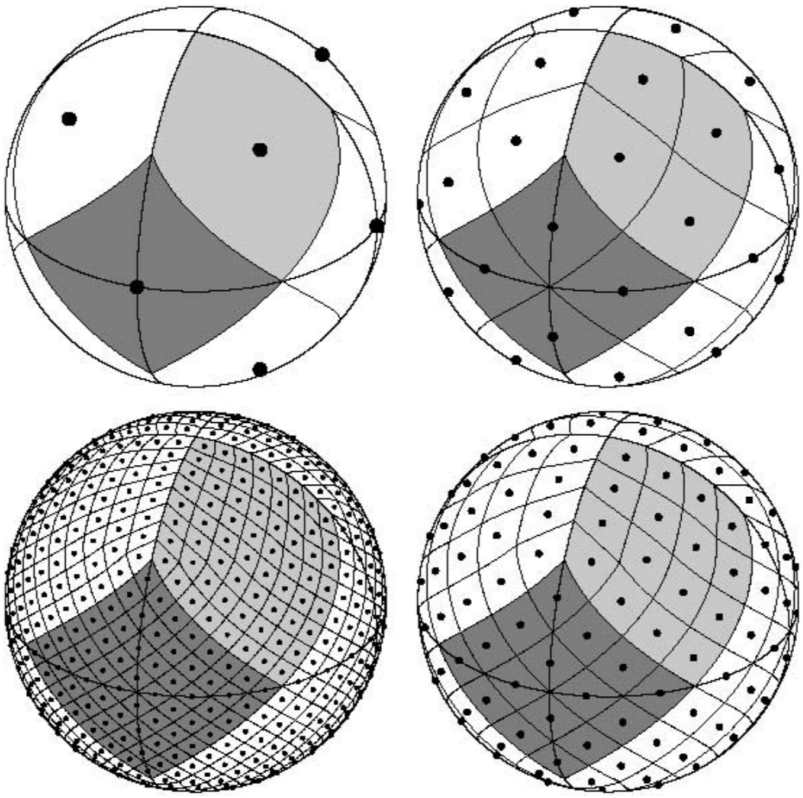

Figure 4: Partition of sphere into increasing number of pixels via HEALPix.

However, HEALPix is not entirely perfect. Often in astronomical observation of some event, the region of the event tends to appear at a small part of the map, such as Figure 5. In this case, having the same pixel density seems unnecessary and uses a lot of space as majority part of the skymap has a density of zero. This is when MOC (Multi Order Coverage) becomes convenient. Figure 6 shows a high pixel density at the area of interest and low pixel density at other area. Compare with Figure 4.

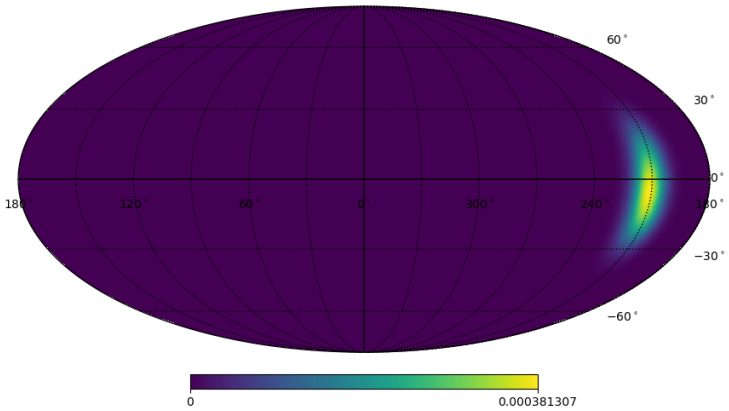

Figure 5: A skymap of a single neutrino detected by IceCube, the intensity of the colour corresponds to the probability density of neutrino.

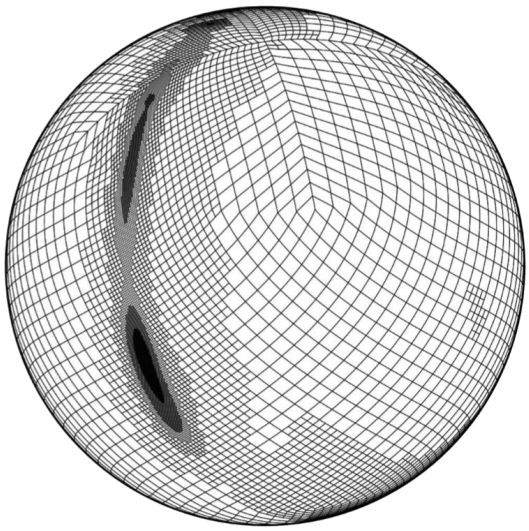

Figure 6: Pixelization when HPMOC is in use.

The combination of HEALPix and MOC: HPMOC, is an easy-to-use Python library that makes the analysis and manipulation of skymap much more convenient. See `https://hpmoc.stc.sh/` for more details.

1.4 Aim

After the above introduction, we can now state the purpose of this internship. The current version of LLAMA supports only two joint messengers detection, namely high-energy neutrinos from IceCube and gravitational-waves from LIGO. The need for an upgrade to LLAMA is rising as more and more detectors become available. In this report, we will describe how to add a new messenger: GRB to the existing GW-Neutrino joint detection. We will first develop a general framework for any number of messengers and then consider the particular case of these three messengers.

2 Theoretical Model

2.1 Hypothesis Counting

We will start by claiming that any messenger detected is either a *noise* or a true *signal* from a source, and any two signals are either from the same source or different sources. Then we would have all sorts of distinct possibilities. Each possibility is a statistical hypothesis. We will explain with two particular cases of two and three messengers by tabulation. Table 1 is the case of two messengers M_1 and M_2 with five possibilities. Note that when both of them are signals, they might be from the same source or different sources.

M_1	M_2
noise	noise
signal	noise
noise	signal
signal from source 1	signal from source 2
signal from same source	signal from same source

Table 1: Possible combinations for 2 messengers.

Table 2 then elaborates 15 possibilities if there're three messengers. A cross sign indicates noise and a check sign indicates signal. The number in the subscript of the check sign in each row is only an

indication of whether the messengers are from the same source (same number) or not (different numbers). The numbers themselves carry no other meaning. Only the last row suggests that the three messengers all come from the same source.

	M_1	M_2	M_3
1	×	×	×
2	×	✓	×
3	×	×	✓
4	×	$✓_1$	$✓_1$
5	×	$✓_1$	$✓_2$
6	✓	×	×
7	$✓_1$	×	$✓_1$
8	$✓_1$	×	$✓_2$
9	$✓_1$	$✓_1$	×
10	$✓_1$	$✓_2$	×
11	$✓_1$	$✓_2$	$✓_3$
12	$✓_1$	$✓_1$	$✓_2$
13	$✓_1$	$✓_2$	$✓_2$
14	$✓_1$	$✓_2$	$✓_1$
15	$✓_1$	$✓_1$	$✓_1$

Table 2: Possible combinations for 3 messengers.

2.1.1 Stirling and Bell numbers

The above counting is a more general combinatorics problem of distributing n *distinct objects into* n *identical non-empty bins*, or equivalently speaking, it counts the number of ways a set of n elements can be partitioned up to n non-empty sets. Such number B_n, is known as the *Bell number* [16]. It has the following recursive relation:

$$B_{n+1} = \sum_{k=0}^{n} \binom{n}{k} B_k \tag{1}$$

where $B_0 = 1$. This relation is not hard to prove. Consider the extra one element different from B_{n+1} and B_n. Suppose there are k elements not in the set where this element is in, then there are $\binom{n}{k}$ ways to choose these k elements and B_k ways to partition them into non-empty sets. Summing the product over all possible k gives B_{n+1}.

$B_3 = 5, B_4 = 15$ also agrees with the above two tables. Notice that B_{n+1} (not B_n) denotes the number of possible combinations for n messengers, because there is an extra bin of noise messenger.

Alternatively, one can use *Stirling number of the second kind* [17] $S(n, k)$ to represent Bell number:

$$B_n = \sum_{k=1}^{n} S(n, k) \tag{2}$$

This is because the Stirling number $S(n, r)$ denotes the number of ways a set of n elements can be partitioned into r non-empty sets and it also follows a recursive relation:

$$S(n, r) = rS(n-1, r) + S(n-1, r-1) \tag{3}$$

2.2 Hypothesis Testing

Now that we know how to enumerate all possible hypotheses, the idea of finding coincidental signals is converted into a hypothesis testing between *signal* and *null* hypothesis. Here odds ratio is used to

quantify this. The whole framework is based on Bayesian statistics [12]. Here I list a few important probability identities that will be used in the upcoming derivations. The notations are: A, B are random events, x for measurement, H for hypothesis, H_α for sub-hypothesis, θ for prior.

For conditional probabilities:

$$P(A \cap B) \equiv P(A, B) = P(A|B)P(B) = P(B|A)P(A) \tag{4}$$

Bayes' rule (invert conditional probability):

$$P(A|B) = \frac{P(B|A)P(A)}{P(B)} \tag{5}$$

This is in fact equivalent to the right-half of Eq. (4)

Sum of the distinct sub-hypotheses:

$$P(H) = \sum_k P(H_k) \tag{6}$$

Decomposition of probability:

$$P(x) = \sum_k P(x|H_k)P(H_k) \quad \text{discrete} \tag{7}$$

$$P(x) = \int P(x|\theta)P(\theta)d\theta \quad \text{continuous} \tag{8}$$

Now prove that

$$P(x|H) = \frac{\sum_k P(x|H_k)P(H_k)}{\sum_k P(H_k)} \tag{9}$$

Since

$$P(x|H) = \frac{P(x \cap H)}{P(H)} \tag{10}$$

One only need to prove that the numerators are equal:

$$\begin{aligned}
P(x \cap H) &= \sum_k P((x \cap H)|H_k)P(H_k) \\
&= \sum_k \frac{P(x \cap H \cap H_k)}{\cancel{P(H_k)}}\cancel{P(H_k)} \\
&= \sum_k P(x \cap H \cap H_k) \\
&= \sum_k P(x \cap H_k) \qquad \text{because } H_k \subset H \\
&= \sum_k P(x|H_k)P(H_k) \quad \blacksquare
\end{aligned}$$

With Eq. (9) and Bayes' rule, the odds ratio of concern is

$$\frac{P(H_s|x)}{P(H_n|x)} = \frac{\sum_i P(x|H_s^i)P(H_s^i)}{\sum_j P(x|H_n^j)P(H_n^j)} \tag{11}$$

s and n represent signal and null hypothesis. Superscripts are their sub-hypotheses. On the right of the above equation is the ratio of the probabilities of signal and null hypotheses given the measurement. In the case of Table 2, H_s contains only the last row and H_n contains all the remaining hypotheses.

Therefore, $P(x|H_k), \forall k$ must be known to find the odds ratio:

$$P(x|H_k) = \int P(x|\theta, H_k)P(\theta|H_k)d\theta \tag{12}$$

$$\Rightarrow P(x|H_k)P(H_k) = \int P(x|\theta, H_k) \underbrace{P(\theta|H_k)P(H_k)}_{\text{Invert with Bayes' rule}} d\theta \tag{13}$$

$$\Rightarrow P(x|H_k)P(H_k) = \int \underbrace{P(x|\theta, H_k)}_{A} \underbrace{P(H_k|\theta)}_{B} \underbrace{P(\theta)}_{C} d\theta \tag{14}$$

Calculation of odds ratio is then confined to finding these three terms A,B,C.

There are several detectors in multi-messenger detection. Consider an independent detector α resulting in measurement x_α, this decomposes term A,

$$P(x|\theta, H_k) = \prod_\alpha P(x_\alpha|\theta, H_k), \quad \forall x_\alpha \subset x \tag{15}$$

$$P(x_\alpha|\theta, H_k) = \sum_{\xi \subset x_\alpha} \underbrace{P(x_\alpha|\theta, H_k, \xi)}_{\blacktriangle} \underbrace{P(\xi|\theta, H_k)}_{\bigstar} \tag{16}$$

ξ is a subset of x_α ($\xi \subset x_\alpha$), it satisfies all different possibilities within x_α. Its summation should have $\binom{|x_\alpha|}{|\xi|}$ terms, where $|x_\alpha|, |\xi|$ denote the number of elements in the corresponding set.

Suppose

$$\xi = \{\underbrace{x^1_{\alpha_1} \dots x^{n_1}_{\alpha_1}}_{\text{source 1}}; \dots; \underbrace{x^1_{\alpha_m} \dots x^{n_m}_{\alpha_m}}_{\text{source m}}\} \tag{17}$$

Notation: $\boxed{x^l_{\alpha_k}}$ source $\#k$ and detected particle/signal $\#l$

Then for term $\blacktriangle$,

$$\begin{aligned} P(x_\alpha|\theta, H_k, \xi) &= P(x_{\alpha_1}, \dots, x_{\alpha_m}|\theta, H_k) \\ &= P(x_{\alpha_1}|\theta_1, H_k) \cdots P(x_{\alpha_m}|\theta_m, H_k) \\ &= \prod_{r=1}^{m} P(x_{\alpha_r}|\theta_r, H_k) \end{aligned} \tag{18}$$

And for term $\bigstar$,

$$P(\xi|\theta, H_k) = \left(\prod_{r=1}^{m} \binom{n_r}{W}\right)^{-1} \tag{19}$$

where W is the number of detections made.

Combining all the above and expand like Eq.(11),

$$\sum_s P(x|H_k)P(H_k) =$$

$$\sum_s \int_\theta \prod_\alpha \prod_{r=1}^{m} P(x_{\alpha_r}|\theta_r, H_k)\, P(H_k|\theta)\, P(\theta)\, d\theta \cdot \binom{|x_\alpha|}{|\xi|} \left(\prod_{r=1}^{m} \binom{n_r}{W}\right)^{-1} \quad \blacksquare \tag{20}$$

Evidently, all that needed to find the odds ratio are these three terms:

$$P(x_{\alpha_r}|\theta_r, H_k) \quad P(H_k|\theta) \quad P(\theta) \tag{21}$$

The above derivation is a general statistical model for any number of messengers, any number of independent detectors, any number of detected signals and any number of sources. In practice, one will have to specify priors θ and measurements x in detail based on the detector property and the type of signals it detects. In what follows we will start to implement the third messenger GRB into LLAMA. This is a non-trivial process containing complicated and delicate manipulation of data and careful handling of the code.

3 Implementation

3.1 A Background Cascade Simulation

The IceCube detector usually categorises the detected neutrino events into either *tracks* or *cascades* (or *double-cascades* in rare cases) according to their detected morphologies [1]. This is due to the working principle of IceCube: by observing the emitted Cherenkov light. Such light is emitted when incoming neutrinos interact with the ice and produce relativistic charged particles such as muons and electrons, which subsequently radiate for the photomultiplier tubes (PMT) to detect. The detector is filled up with PMT and it could potentially trace the trajectory of an interacting neutrino. When the neutrino leaves a tracklike morphology, i.e. a long narrow tail of light emission in a certain direction, such event is called a track. Similarly when the interaction makes an electromagnetic (and) or hadronic shower, the event is a cascade. The characteristics of these two events are that cascades have higher localized energy deposition whereas tracks have more precise sky localization, as evident from their respective morphologies.

As described earlier, the coincidental significance search is quantified by a ratio of probabilities of signal and null hypotheses. The latter, contains the hypotheses that some or all of the messengers may be noise or *background*. In the case of neutrino detection, the background neutrinos would mostly be solar neutrinos coming from the sun and atmospherical muons that impersonate the outgoing muons of real neutrinos interacting with ice. These are considered as background since we are dealing with high energy neutrinos from astrophysical sources.

A common way to quantify background is to use empirical data and it will be accomplished by a simulation. For cascades, the IceCube high-energy starting event (HESE) sample [1] are used here. It has 7.5 years of data until 2021 which contains only 102 events: 71 cascades, 27 tracks, 4 double-cascades. Fortunately it has a reconstructed Monte-Carlo simulated data based on it with 821764 events. The three tables below give a glimpse into the data aforementioned.

Table 3: HESE Data

recoDepositedEnergy	recoMorphology	recoZenith	recoLength
40094.570312	0	1.827070	NaN
98474.578125	0	1.422724	NaN
70592.507812	1	0.955265	NaN
184547.453125	0	0.912687	NaN
101133.023438	0	0.891402	NaN
60871.656250	1	1.289066	NaN
41134.148438	0	0.433679	NaN
22613.667969	0	1.906153	NaN
114974.000000	0	2.592699	NaN

Table 4: HESE Monte Carlo Observable Data

recoDepositedEnergy	recoLength	recoZenith	recoMorphology
205266.250000	NaN	2.296108	0
70989.992188	NaN	1.222855	0
42118.488281	NaN	0.588104	0
196890.750000	NaN	1.273115	1
92714.117188	NaN	1.182715	1
133442.031250	NaN	0.119648	1

Table 5: HESE Monte Carlo Truth Data

primaryType	primaryZenith	primaryEnergy	weightOverFluxOverLivetime	interactionType
12	2.422330	464800.948806	3.185172e+06	2
12	0.879347	134045.497279	8.563087e+05	2
12	0.691149	50542.826319	1.033216e+05	1
13	1.351471	623849.869823	0.000000e+00	0
13	1.148815	268162.026821	0.000000e+00	0
13	1.278967	549664.260228	0.000000e+00	0
13	1.157839	127729.523306	0.000000e+00	0
13	0.158745	152825.460789	0.000000e+00	0

Energy is in the unit of GeV and zenith is in unit of radians in the coordinate of IceCube detector. Unit conversion of coordinates has to be carried out since for most other astronomical detectors such as LIGO and Fermi in our case, equatorial coordinates with declination (DEC) and right ascension (RA) are used but for IceCube, horizontal coordinates centred at the detector with zenith and azimuth are used. The coordinate conversion between declination and zenith is about 90° difference because the IceCube happens to be situated close to the south pole. This is a convenient approximation with little error. A more precise transformation between the two coordinate systems requires the knowledge of time, due to Earth precession. Morphologies of 0, 1 and 2 correspond to cascades, tracks and double cascades. Only those with zero values are selected. The difference of zeniths between observable and truth data are considered as one standard deviation of neutrino's sky localisation. Figure 7 plots the 2D histograms of simulated cascade data and scatters of real HESE events and the more recent AMON IceCube cascades event from `https://gcn.gsfc.nasa.gov/amon_icecube_cascade_events.html` for comparison. The plot says that most neutrinos seem to come from south pole, which is a result from the location of IceCube and that the neutrinos coming from north have to travel a longer path through earth.

The simulation used HESE sample of cascades together with sub-threshold gravitational-wave events fed into LLAMA program to generate about 10,000 odds ratios. Neutrino times are uniformly distributed in a 500s time window around the corresponding GW event. RAs are also uniformly randomized. The resulted odds ratios is plotted in Figure 8 as a histogram. As one would expect, almost all of them are well under the value of 1. This simulation would then help us with the coincident significance search with cascades as one of the messengers, since it provides an empirical null hypotheses likelihood estimate.

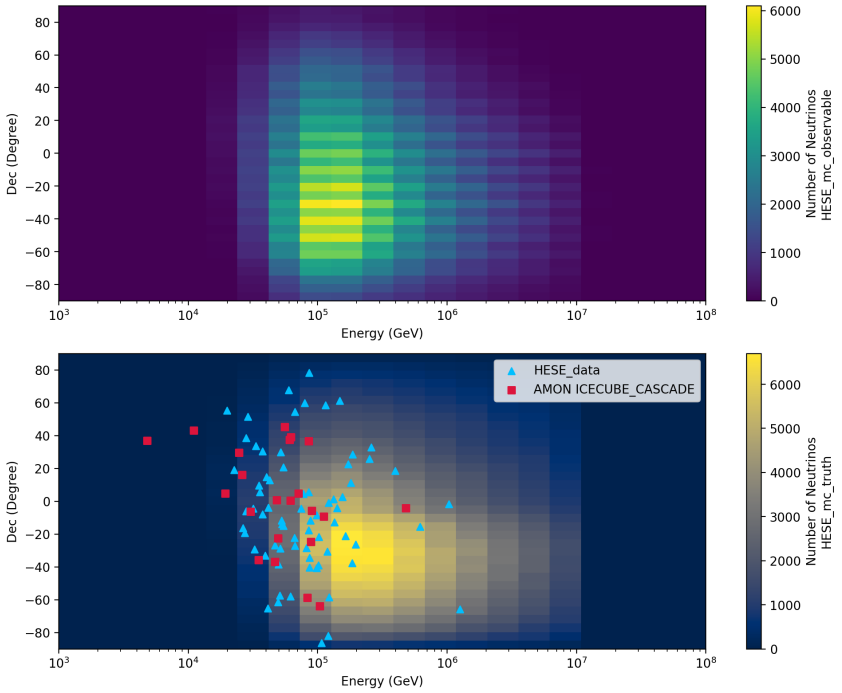

Figure 7: Histogram displaying the data from MC simulated HESE neutrino cascades.

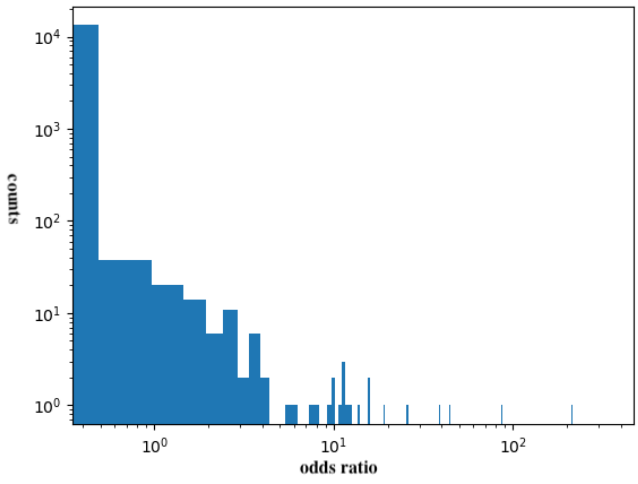

Figure 8: Generated odds ratios in histogram.

3.2 GW-Neutrino-GRB Significance Calculation

This subsection is used to deduce the three terms in Eq. (21) for this particular three messengers. Therefore, the exact details of the detected messengers must be specified. It starts with the variables of measurements x and priors θ below.

Variables

$$
\begin{aligned}
x_{\mathrm{gw}} &= \{t_{\mathrm{gw}}, M, \rho, D\} \\
x_{\nu} &= \{t_{\nu}, \Omega_{\nu}, \sigma_{\nu}, \epsilon_{\nu}\} \\
x_{\gamma} &= \{t_{\gamma}, S, \mathcal{E}\} \\
\theta &= \{t_s, r_s, \Omega_s, E_{\mathrm{gw}}, E_{\nu}, E_{\gamma}, \kappa_{\gamma}\}
\end{aligned}
$$

Undoubtedly, Each measurement must contain a time to record when a event takes place. For x_{gw}, observation result of gravitational-waves, M is the reconstructed sky location probability density distribution (skymap), ρ is the signal to noise ratio (SNR), D is the reconstructed distance distribution. For x_{ν}, high energy neutrinos, the skymap is described by a Gaussian distribution centred at its reconstructed direction Ω_{ν} with standard deviation σ_{ν}:

$$
\frac{1}{2\pi\sigma_{\nu}^2} \mathrm{e}^{-\frac{|\Omega_{\nu}-\Omega|^2}{2\sigma_{\nu}^2}} \tag{22}
$$

The denominator is $\left(\sqrt{2\pi}\sigma_{\nu}\right)^2$ because skymap is two dimensional. A Gaussian distribution is used here for the neutrino skymap due to the indirect observation of neutrinos. ϵ_{ν} is the observed energy. For gamma-ray bursts, S is its skymap and $\mathcal{E}$ is estimated energy. For priors θ, information on the source, r_s, Ω_s are its distance and sky position. $E_{\mathrm{gw}}, E_{\nu}, E_{\gamma}$ are energies. κ_{γ} is a parameter for GRB defined as the ratio of peak flux and fluence (flux integrated over the burst duration). The GRBs sweep through the Earth like gravitational-waves and there is no observed energy like neutrinos since the detector can only detect a portion of photons at any time. Hence κ_{γ} is a more comparable quantity to energy and used here [13] [10] [14] [7].

First we study the prior probability distribution $P(\theta)$. Assume that a messenger is equally likely to occur at any time during the observation period Δt and Δt is independent of any other parameters:

$$
P(t_s) = \frac{1}{\Delta t} \tag{23}
$$

Assume the universe has a uniform distribution of sources, then for distance:

$$
P(r) \propto r^2 \tag{24}
$$

the power of two on r comes from the volume element in space, $dV \propto r^2 dr$. In addition, the antenna pattern of GW detectors can be considered too:

$$
f_A\left(\mathbf{\Omega}, t_{\mathrm{gw}}\right) = \sqrt{\sum_k F_{k,+}\left(\psi, \mathbf{\Omega}, t_{\mathrm{gw}}\right)^2 + F_{k,\times}\left(\psi, \mathbf{\Omega}, t_{\mathrm{gw}}\right)^2} \tag{25}
$$

where F are the responses of antenna in two polarization and ψ is the inclined angle of GW emission with respects to the plane of detectors.

Energy dependence is assumed as

$$
P(E_{\mathrm{gw}}, E_{\nu}, \kappa_{\gamma}) \propto \frac{1}{E_{\mathrm{gw}}} \cdot \frac{1}{E_{\nu}} \cdot \frac{1}{\kappa_{\gamma}} \tag{26}
$$

for energies in the range of $[E_{\mathrm{gw}}^-, E_{\mathrm{gw}}^+]$ and $[E_{\nu}^-, E_{\nu}^+]$. This is the empirical maximum and minimum range. Note that E_{gw} is not a directly measurable quantity. It is related to signal-to-noise ratio ρ

$$
E_{\mathrm{gw}} = \left(\frac{\rho D}{k_0}\right)^2 \tag{27}
$$

where k_0 is some constant. This is due to the proportionality of SNR and energy per unit area:

$$
\rho \propto \sqrt{\frac{E}{4\pi D^2}} \tag{28}
$$

The independence of each parameter allows us to combine the above to give

$$P(\theta) = \frac{r^2}{\Delta t \cdot E_{\rm gw} \cdot E_\nu \cdot \kappa_\gamma} \tag{29}$$

It is safe to ignore the proportional/normalization constant since they cancel in Eq. (11).

The next term to study is $P(H_k|\theta)$, probability of a hypothesis given source parameter. It depends on the expected count of a multi-messenger event. To take the example of a signal hypothesis H_s^n where there are n coincident neutrinos.

$$P(H_s^n|\theta) = \dot{n}_{\rm gw+\nu+\gamma}\, \Delta t\, \text{Poisson}(n, \langle n_\nu(E_\nu, r, \Omega)\rangle\ ) \tag{30}$$

$\dot{n}_{\rm gw+\nu+\gamma}$ is the total multi-messenger event rate of the whole universe bounded by the maximum distance allowed for detectors. Poisson distribution with an expected observed neutrino number n and mean $\langle n_\nu(E_\nu, r, \Omega)\rangle$ is used to represent probability of detecting n neutrinos. Expected number of detected neutrinos given emission energy, sky location and distance is [3]

$$\langle n_\nu(E_\nu, r, \Omega)\rangle = n_{\nu,51,100}(\Omega)\left(\frac{E_\nu}{10^{51}\text{erg}}\right)\left(\frac{r}{100\text{Mpc}}\right)^{-2} \tag{31}$$

where $n_{\nu,51,100}(\Omega)$ is a detector-dependent variable approximately 1.1 for IceCube.

Now comes the most significant terms $P(x_{\alpha_r}|\theta_r, H_k)$. For GW, expand as follows

$$P(x_{\rm gw}|\theta, H_s) = P(t_{\rm gw}|\theta, H_s) \cdot P(\rho|t_{\rm gw}, \theta, H_s) \cdot P(M|t_{\rm gw}, \rho, \theta, H_s) \cdot P(D|M, t_{\rm gw}, \rho, \theta, H_s) \tag{32}$$

Such expansion will be used many times in the deduction. It is simply a variant of Bayes' rule for probabilities of many parameters:

$$P(A, B, C|X, Y) = P(A|B, C, X, Y)P(B, C|X, Y) \tag{33}$$

$$= P(A|B, C, X, Y)P(B|C, X, Y)P(C|X, Y) \tag{34}$$

For the first term in Eq. (32), $t_g w$ has no dependencies in θ other than t_s. We use the same assumption in Eq. (23)

$$P(t_{\rm gw}|t_s, H_s) = \frac{1}{t_{\rm gw}^+ - t_{\rm gw}^-} \tag{35}$$

For the second term on $\rho_{\rm gw}$, an appropriate representation would be a delta function δ

$$P(\rho|t_{\rm gw}, \theta, H_s) = \delta\left[\rho_{\rm gw} - N\sqrt{E_{\rm gw}} r^{-1} f_A\right] \tag{36}$$

The third term is inverted as

$$P(M|t_{\rm gw}, \rho, \theta, H_s) = \frac{P(\theta|M, t_{\rm gw}, \rho, H_s) \cdot \cancel{P(M|t_{\rm gw}, \rho, H_s)}}{P(\theta|t_{\rm gw}, \rho, H_s)} \tag{37}$$

but since skymap M has no connection to hypothesis H_s, hence $P(M|t_{\rm gw}, \rho, H_s) = P(M|t_{\rm gw}, \rho)$ and will be cancelled in the null hypothesis. The remaining term is simplified as

$$P(M|t_{\rm gw}, \rho, \theta, H_s) = \frac{P(\theta|M, t_{\rm gw}, \rho, H_s)}{P(\theta|t_{\rm gw}, \rho, H_s)} = \frac{M}{f_A} \tag{38}$$

For the last term

$$P(D|M, t_{\rm gw}, \rho, \theta, H_s) = \frac{P(\theta|M, t_{\rm gw}, \rho, D, H_s) \cdot \cancel{P(D|M, t_{\rm gw}, \rho, H_s)}}{P(\theta|M, t_{\rm gw}, \rho, H_s)} \tag{39}$$

$$= D\frac{N}{r^2 \times r^{-1}} \tag{40}$$

where r^2 is due to prior probability and r_{-1} is due to Eq. (27). Combine all above equations,

$$P(x_{\rm gw}|\theta, H_s) = N\,\delta\Big[\rho_{\rm gw} - N\sqrt{E_{\rm gw}}r^{-1}f_A\Big]\,\frac{M}{f_A}\,\frac{D}{r(t^+_{\rm gw} - t^-_{\rm gw})} \tag{41}$$

One can get the equation for neutrinos via a similar procedure and get

$$P(x_\nu|\theta, H_s) = N\,A_{\rm eff}(\epsilon_\nu, \Omega)\,\frac{1}{2\pi\sigma^2_\nu}e^{-\frac{|\Omega_\nu - \Omega|^2}{2\sigma^2_\nu}}\frac{1}{\epsilon_\nu^{-2}\cdot(t^+_\nu - t^-_\nu)} \tag{42}$$

$A_{\rm eff}$ is the effective area of IceCube, similar to the antenna pattern of GW detectors. ϵ_ν^{-2} is due to the Fermi processes [15] in which the neutrino spectral density follows a power law of inverse 2, $dN_\nu/d\epsilon_\nu \propto \epsilon_\nu^{-2}$.

For GRB, the detection likelihood is

$$P(x_\gamma|\theta, H_s) = \frac{N}{(1+z(r_s))^4\kappa_\gamma}\frac{1}{t^+_\gamma - t^-_\gamma} \tag{43}$$

It has a simpler formula due to less information the detector can provide. However since GRB is electromagnetic waves, we have to consider the redshift $z(r_s)$). $(1+z(r_s))^4$ accounts for the time dilation from Hubble expansion. The time window for GRB is set to $t^+_\gamma = +250s, t^-_\gamma = -100s$ [5].

3.3 GRB data

The data for gamma-ray burst are retrieved from Fermi Gamma-Ray Space Telescope `https://gcn.gsfc.nasa.gov/fermi_gbm_subthresh_archive.html` and `https://fermi.gsfc.nasa.gov/ssc/data/access/`. Below is an example of a real time Fermi GRB alert.

```
//////////////////////////////////////////////////////////////
TITLE:           GCN/FERMI NOTICE
NOTICE_DATE:     Tue 15 Aug 23 14:15:39 UT
NOTICE_TYPE:     Fermi-GBM Alert
RECORD_NUM:      1
TRIGGER_NUM:     713801737
GRB_DATE:        20171 TJD;   227 DOY;   23/08/15
GRB_TIME:        51332.65 SOD {14:15:32.65} UT
TRIGGER_SIGNIF:  5.5 [sigma]
TRIGGER_DUR:     0.064 [sec]
E_RANGE:         2-2 [chan]   23-47 [keV]
ALGORITHM:       26
DETECTORS:       0,0,0, 1,0,1, 0,0,0, 0,0,0, 0,0,
LC_URL:          http://heasarc.gsfc.nasa.gov/FTP/fermi/data/gbm/triggers/2023/bn230815594/quicklook
COMMENTS:        Fermi-GBM Trigger Alert.
COMMENTS:        This trigger occurred at longitude,latitude = 243.63,-25.62 [deg].
COMMENTS:        The LC_URL file will not be created until ~15 min after the trigger.


//////////////////////////////////////////////////////////////
TITLE:           GCN/FERMI NOTICE
NOTICE_DATE:     Tue 15 Aug 23 14:16:02 UT
NOTICE_TYPE:     Fermi-GBM Flight Position
RECORD_NUM:      45
TRIGGER_NUM:     713801737
GRB_RA:          116.650d {+07h 46m 36s} (J2000),
116.950d {+07h 47m 48s} (current),
116.014d {+07h 44m 03s} (1950)
```

```
GRB_DEC:          -1.033d {-01d 01' 59"} (J2000),
-1.093d {-01d 05' 32"} (current),
-0.910d {-00d 54' 34"} (1950)
GRB_ERROR:       38.37 [deg radius, statistical plus systematic]
GRB_INTEN:       29 [cnts/sec]
DATA_SIGNIF:     3.90 [sigma]
INTEG_TIME:      4.096 [sec]
GRB_DATE:        20171 TJD;   227 DOY;   23/08/15
GRB_TIME:        51332.65 SOD {14:15:32.65} UT
GRB_PHI:          11.00 [deg]
GRB_THETA:        65.00 [deg]
DATA_TIME_SCALE: 4.0960 [sec]
HARD_RATIO:      0.00
LOC_ALGORITHM:   3 (version number of)
MOST_LIKELY:     100%  Unreliable location
2nd_MOST_LIKELY:   0%  n/a
DETECTORS:       0,0,0, 1,0,1, 0,0,0, 0,0,0, 0,0,
SUN_POSTN:       144.87d {+09h 39m 28s}  +14.01d {+14d 00' 27"}
SUN_DIST:         31.51 [deg]   Sun_angle= 1.9 [hr] (West of Sun)
MOON_POSTN:      137.68d {+09h 10m 43s}  +21.31d {+21d 18' 24"}
MOON_DIST:        30.20 [deg]
MOON_ILLUM:      1 [%]
GAL_COORDS:      220.25, 11.76 [deg] galactic lon,lat of the burst (or transient)
ECL_COORDS:      118.89,-21.84 [deg] ecliptic lon,lat of the burst (or transient)
LC_URL:          http://heasarc.gsfc.nasa.gov/FTP/fermi/data/gbm/triggers/2023/bn230815594/quicklook
COMMENTS:        Fermi-GBM Flight-calculated Coordinates.
COMMENTS:        This trigger occurred at longitude,latitude = 243.63,-25.62 [deg].
COMMENTS:        The LC_URL file will not be created until ~15 min after the trigger.
```

The following are headers in the data containing HEALPIX skymap (last row) and detailed information regarding the detected event. See Appendix A for details on them.

```
Filename: /Users/easy/llama/grb/trigger/glg_trigdat_all_bn230817315_v00.fit
No.    Name      Ver    Type      Cards   Dimensions   Format
0  PRIMARY       1 PrimaryHDU      49   ()
1  TRIGRATE      1 BinTableHDU     48   1R x 5C   [1D, 1D, 4E, 3E, 112E]
2  BCKRATES      1 BinTableHDU     46   1R x 4C   [1D, 1D, 2B, 112E]
3  OB_CALC       1 BinTableHDU     74   1R x 15C   [1D, 1E, 1E, 1E, 1I, 2I, 2E, 1E, 1E, 1E, 1E, 12I,
4  MAXRATES      1 BinTableHDU     49   1R x 5C   [1D, 1D, 4E, 3E, 112E]
5  EVNTRATE      1 BinTableHDU     49   153R x 5C   [1D, 1D, 4E, 3E, 112E]


Filename: /Users/easy/llama/grb/burst/glg_healpix_all_bn230101095.fit
No.    Name      Ver    Type      Cards   Dimensions   Format
0  PRIMARY       1 PrimaryHDU      43   ()
1  HEALPIX       1 BinTableHDU     58   192R x 2C   [1024E, 1024E]
```

Below are two skymaps from Fermi telescopes. Purple area are the probability density function for GRB. One is a triggered burst with much more precise localisation than the other one of sub-threshold. The grey areas are where the different detectors face towards. Black lines are contour lines with different confidence levels.

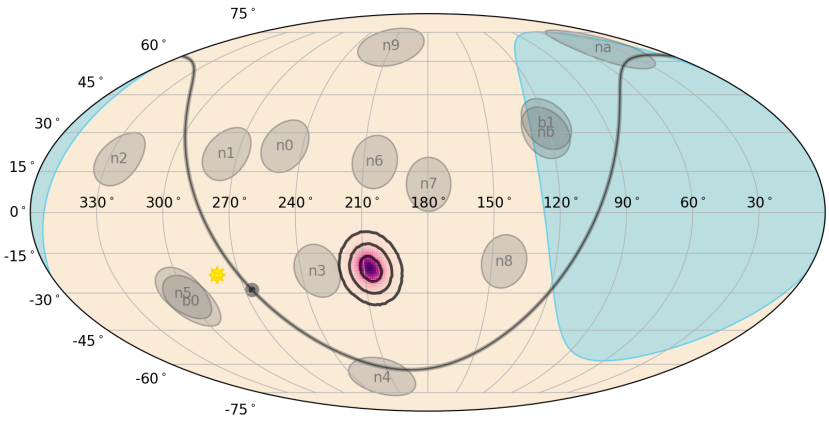

Figure 9: GRB skymap from Fermi telescope.

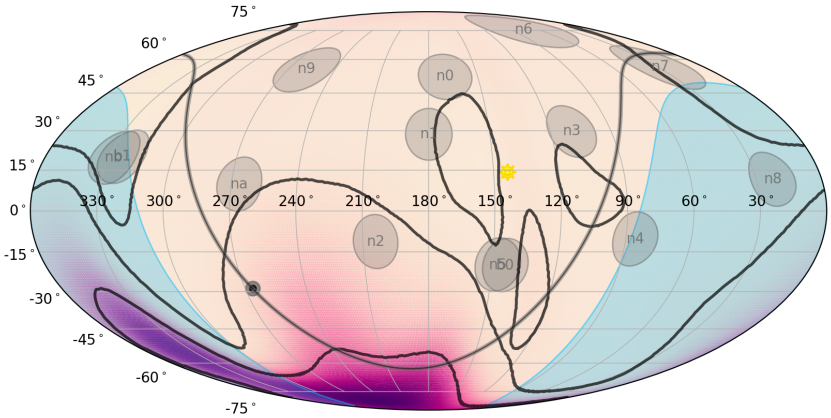

Figure 10: GRB sub-threshold skymap from Fermi telescope.

The algorithm in LLAMA is updated following the calculation in Section 3.2. It maybe worthwhile to emphasize that the equations derived does not seem to consider how the localisations of different messengers are taken into account. After all, this is the most obvious way to tell if different messengers are from the same source. This is explicitly done in the LLAMA by **multiplying** different skymaps via HPMOC.

4 Conclusion

We have upgraded the multi-messenger algorithm LLAMA to accept GRBs for coincident significance search. However, due to the large amount of data processing involved, a "sanity check" is important to make sure the program gives right results. This is done in the table shown below by changing various parameters of GRB including localization, κ_γ and time difference to observe if the output odds ratio makes sense. This is only a preliminary check, further analysis by changing the parameters of GW and neutrinos also needs to be conducted.

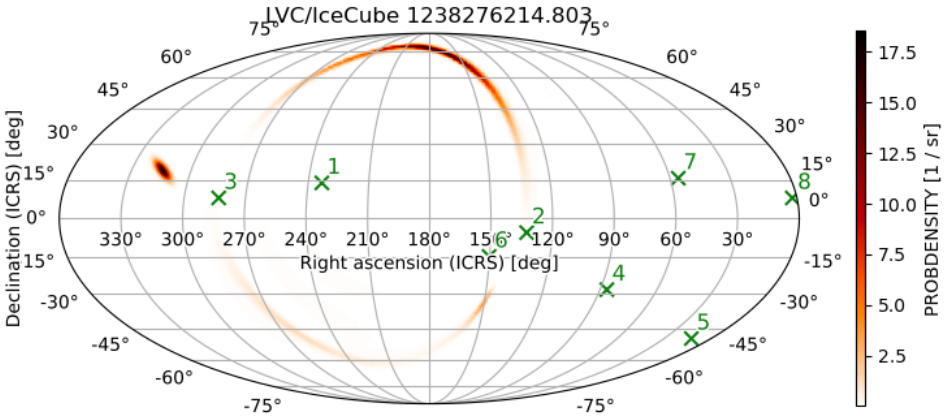

Figure 11: Skymaps of neutrinos, GW and GRB on the same map.

Table 6: Sanity Check

Case	RA (deg)	Dec (deg)	Kappa	t-grb - t-GW [s]	GPS time	Odds ratio
1	313.418	7.745	5000	10	1248331538.5292	0.00228
2	310.918	7.745	5000	10	1248331538.5292	0.00123
3	305.918	7.745	5000	10	1248331538.5292	1.603e-05
4	298.418	7.745	5000	10	1248331538.5292	4.359e-08
5	283.418	7.745	5000	10	1248331538.5292	1.437e-20
6	315.918	7.745	5000	10	1248331538.5292	0.00145
7	320.918	7.745	5000	10	1248331538.5292	3.448e-05
8	328.418	7.745	5000	10	1248331538.5292	1.891e-09
9	343.418	7.745	5000	10	1248331538.5292	5.515e-24
10	313.418	10.745	5000	10	1248331538.5292	0.00149
11	313.418	15.745	5000	10	1248331538.5292	0.00055
12	313.418	20.745	5000	10	1248331538.5292	4.413e-05
13	313.418	27.745	5000	10	1248331538.5292	6.202e-08
14	313.418	4.745	5000	10	1248331538.5292	0.00123
15	313.418	-0.255	5000	10	1248331538.5292	8.902e-05
16	313.418	-5.255	5000	10	1248331538.5292	3.130e-07
17	313.418	-12.255	5000	10	1248331538.5292	2.593e-10
18	307.418	4.745	500	10	1248331538.5292	1.879e-06
19	307.418	4.745	1000	10	1248331538.5292	5.005e-06
20	307.418	4.745	10000	10	1248331538.5292	0.000137
21	307.418	4.745	100000	10	1248331538.5292	0.001812
22	307.418	4.745	200000	10	1248331538.5292	0.004571
23	307.418	4.745	5000	-300	1248331228.5292	3.171e-05
24	307.418	4.745	5000	-100	1248331428.5292	6.343e-05
25	307.418	4.745	5000	1	1248331529.5292	7.913e-05
26	307.418	4.745	5000	100	1248331628.5292	6.343e-05
27	307.418	4.745	5000	300	1248331828.5292	3.171e-05
28	307.418	4.745	5000	10	1248331538.5292	1.632e-05
29	307.418	4.745	5000	10	1248331538.5292	0.0001366
30	307.418	4.745	5000	10	1248331538.5292	0.0002405
31	307.418	4.745	5000	10	1248331538.5292	8.065e-05
32	307.418	4.745	5000	10	1248331538.5292	8.056e-05
33	307.418	4.745	5000	10	1248331538.5292	7.205e-05
34	307.418	4.745	5000	10	1248331538.5292	3.676e-05
35	307.418	4.745	5000	10	1248331538.5292	1.157e-05
36	307.418	4.745	5000	10	1248331538.5292	6.867e-06
37	307.418	4.745	5000	10	1248331538.5292	6.292e-06
38	307.418	4.745	5000	10	1248331538.5292	6.239e-06
39	320.977	21.703	5000	10	1248331538.5292	1.218e-05
40	320.977	21.703	5000	10	1248331538.5292	1.250e-05
41	320.977	21.703	5000	10	1248331538.5292	1.328e-05
42	320.977	21.703	5000	10	1248331538.5292	1.539e-05
43	320.977	21.703	5000	10	1248331538.5292	1.798e-05
44	320.977	21.703	5000	10	1248331538.5292	1.916e-05
45	320.977	21.703	5000	10	1248331538.5292	2.188e-05

References

[1] R. Abbasi, M. Ackermann, J. Adams, J. Aguilar, M. Ahlers, M. Ahrens, C. Alispach, A. Alves Jr, N. Amin, K. Andeen, et al., *Icecube high-energy starting event sample: Description and flux characterization with 7.5 years of data*, Physical Review D, 104 (2021), p. 022002.

[2] B. P. Abbott, R. Abbott, T. Abbott, F. Acernese, K. Ackley, C. Adams, T. Adams, P. Addesso, R. Adhikari, V. B. Adya, et al., *Gw170817: observation of gravitational waves from a binary neutron star inspiral*, Physical review letters, 119 (2017), p. 161101.

[3] A. Albert, M. André, M. Anghinolfi, M. Ardid, J.-J. Aubert, J. Aublin, T. Avgitas, B. Baret, J. Barrios-Martí, S. Basa, et al., *Search for multimessenger sources of gravitational waves and high-energy neutrinos with advanced ligo during its first observing run, antares, and icecube*, The Astrophysical Journal, 870 (2019), p. 134.

[4] W. D. Arnett, J. N. Bahcall, R. P. Kirshner, and S. E. Woosley, *Supernova 1987a*, Annual review of Astronomy and Astrophysics, 27 (1989), pp. 629–700.

[5] B. Baret, I. Bartos, B. Bouhou, A. Corsi, I. Di Palma, C. Donzaud, V. Van Elewyck, C. Finley, G. Jones, A. Kouchner, et al., *Bounding the time delay between high-energy neutrinos and gravitational-wave transients from gamma-ray bursts*, Astroparticle Physics, 35 (2011), pp. 1–7.

[6] I. Bartos, D. Veske, A. Keivani, Z. Márka, S. Countryman, E. Blaufuss, C. Finley, and S. Márka, *Bayesian multimessenger search method for common sources of gravitational waves and high-energy neutrinos*, Physical Review D, 100 (2019), p. 083017.

[7] P. N. Bhat, C. A. Meegan, A. Von Kienlin, W. S. Paciesas, M. S. Briggs, J. M. Burgess, E. Burns, V. Chaplin, W. H. Cleveland, A. C. Collazzi, et al., *The third fermi gbm gamma-ray burst catalog: the first six years*, The Astrophysical Journal Supplement Series, 223 (2016), p. 28.

[8] S. Countryman, A. Keivani, I. Bartos, Z. Marka, T. Kintscher, R. Corley, E. Blaufuss, C. Finley, and S. Marka, *Low-latency algorithm for multi-messenger astrophysics (llama) with gravitational-wave and high-energy neutrino candidates*, arXiv preprint arXiv:1901.05486, (2019).

[9] K. M. Gorski, E. Hivon, A. J. Banday, B. D. Wandelt, F. K. Hansen, M. Reinecke, and M. Bartelmann, *Healpix: A framework for high-resolution discretization and fast analysis of data distributed on the sphere*, The Astrophysical Journal, 622 (2005), p. 759.

[10] D. Gruber, A. Goldstein, V. W. von Ahlefeld, P. N. Bhat, E. Bissaldi, M. S. Briggs, D. Byrne, W. H. Cleveland, V. Connaughton, R. Diehl, et al., *The fermi gbm gamma-ray burst spectral catalog: four years of data*, The Astrophysical Journal Supplement Series, 211 (2014), p. 12.

[11] L. P. Singer, H.-Y. Chen, D. E. Holz, W. M. Farr, L. R. Price, V. Raymond, S. B. Cenko, N. Gehrels, J. Cannizzo, M. M. Kasliwal, et al., *Supplement:"going the distance: mapping host galaxies of ligo and virgo sources in three dimensions using local cosmography and targeted follow-up"(2016, apjl, 829, l15)*, The Astrophysical Journal Supplement Series, 226 (2016), p. 10.

[12] D. Veske, Z. Márka, I. Bartos, and S. Márka, *How to search for multiple messengers—a general framework beyond two messengers*, The Astrophysical Journal, 908 (2021), p. 216.

[13] A. Von Kienlin, C. Meegan, W. Paciesas, P. Bhat, E. Bissaldi, M. Briggs, E. Burns, W. Cleveland, M. Gibby, M. Giles, et al., *The fourth fermi-gbm gamma-ray burst catalog: A decade of data*, The Astrophysical Journal, 893 (2020), p. 46.

[14] A. Von Kienlin, C. A. Meegan, W. S. Paciesas, P. Bhat, E. Bissaldi, M. S. Briggs, J. M. Burgess, D. Byrne, V. Chaplin, W. Cleveland, et al., *The second fermi gbm gamma-ray burst catalog: the first four years*, The Astrophysical Journal Supplement Series, 211 (2014), p. 13.

[15] E. Waxman and J. Bahcall, *High energy neutrinos from cosmological gamma-ray burst fireballs*, Physical Review Letters, 78 (1997), p. 2292.

[16] E. W. Weisstein, *Bell number*, https://mathworld.wolfram.com/, (2002).

[17] ——, *Stirling number of the second kind*, https://mathworld.wolfram.com/, (2002).

A Appendix

```
trigger/glg_trigdat_all_bn230817315_v00.fit: HDUList[0].header
SIMPLE  =                    T / file does conform to FITS standard
BITPIX  =                    8 / number of bits per data pixel
NAXIS   =                    0 / number of data axes
EXTEND  =                    T / FITS dataset may contain extensions
COMMENT   FITS (Flexible Image Transport System) format is defined in 'Astronomy
COMMENT   and Astrophysics', volume 376, page 359; bibcode: 2001A&A...376..359H
CREATOR = 'GBM_TRIGDAT_Reader.pl V1.29' / Software and version creating file
FILETYPE= 'TRIGDAT '           / Name for this type of FITS file
FILE-VER= '1.0.3   '           / Version of the format for this filetype
TELESCOP= 'GLAST   '           / Name of mission/satellite
INSTRUME= 'GBM     '           / Specific instrument used for observation
OBSERVER= 'Meegan  '           / GLAST Burst Monitor P.I.
ORIGIN  = 'GIOC    '           / Name of organization making file
DATE    = '2023-08-17T07:42:39' / file creation date (YYYY-MM-DDThh:mm:ss UT)
DATE-OBS= '2023-08-17T07:32:41' / Date of start of observation
DATE-END= '2023-08-17T07:41:34' / Date of end of observation
TIMESYS = 'TT      '           / Time system used in time keywords
TIMEUNIT= 's       '           / Time since MJDREF, used in TSTART and TSTOP
MJDREFI =                51910 / MJD of GLAST reference epoch, integer part
MJDREFF = 7.428703703703703D-4 / MJD of GLAST reference epoch, fractional part
TSTART  =     713950361.515924 / [GLAST MET] Observation start time
TSTOP   =     713950894.003690 / [GLAST MET] Observation stop time
DETTYPE = 'BOTH    '           / Detector type: NAI or BGO
DATATYPE= 'TRIGDAT '           / Type of lookup table: CTIME or CSPEC
FILENAME= 'glg_trigdat_all_bn230817315_v00.fit' / Name of this file
TRIGTIME=     713950412.140552 / Trigger time relative to MJDREF, double precisi
OBJECT  = 'UNRELOC230817315'   / Burst name in standard format, yymmddfff
RADECSYS= 'FK5     '           / Stellar reference frame
EQUINOX =               2000.0 / Equinox for RA and Dec
RA_OBJ  =             104.6667 / Calculated RA of burst
DEC_OBJ =              80.9333 / Calculated Dec of burst
ERR_RAD =              32.0667 / Calculated Location Error Radius
TRIGSCAL=                   64 / [ms] Triggered timescale
TRIG_ALG=                   25 / Triggered algorithm number
CHAN_LO =                    2 / Trigger channel: low
CHAN_HI =                    2 / Trigger channel: high
ADC_LO  =                  143 / Trigger channel: low (ADC: 0 - 4095)
ADC_HI  =                  258 / Trigger channel: high (ADC: 0 - 4095)
TRIG_SIG=                  5.8 / Trigger significance (sigma)
GEO_LONG=              14.8333 / [deg] Spacecraft geographical east longitude
GEO_LAT =             -18.7167 / [deg] Spacecraft geographical north latitude
DET_MASK= '01000100000000'     / Triggered detectors: (0-13)
RA_SCX  =             148.5682 / [deg] Pointing of spacecraft x-axis: RA
DEC_SCX =              24.6367 / [deg] Pointing of spacecraft x-axis: Dec
RA_SCZ  =             126.1276 / [deg] Pointing of spacecraft z-axis: RA
DEC_SCZ =             -63.6101 / [deg] Pointing of spacecraft z-axis: Dec
INFILE01= 'GLAST_2023229_073332_VC99_GTRIG.0.00' / Level 0 input data file
CHECKSUM= 'lD9hnC8elC8elC8e'   / HDU checksum updated 2023-08-17T07:42:39
DATASUM = '         0'         / data unit checksum updated 2023-08-17T07:42:39

trigger/glg_trigdat_all_bn230817315_v00.fit: HDUList[1].header
XTENSION= 'BINTABLE'           / binary table extension
```

```
BITPIX  =                    8 / 8-bit bytes
NAXIS   =                    2 / 2-dimensional binary table
NAXIS1  =                  492 / width of table in bytes
NAXIS2  =                    1 / number of rows in table
PCOUNT  =                    0 / size of special data area
GCOUNT  =                    1 / one data group (required keyword)
TFIELDS =                    5 / number of fields in each row
TTYPE1  = 'TIME    '           / Beginning of accumulation, calculated value
TFORM1  = '1D      '           / data format of field: 8-byte DOUBLE
TUNIT1  = 's       '           / physical unit of field
TTYPE2  = 'ENDTIME '           / End of accumulation, same as PCKTTIME
TFORM2  = '1D      '           / data format of field: 8-byte DOUBLE
TUNIT2  = 's       '           / physical unit of field
TTYPE3  = 'SCATTITD'           / Spacecraft attitude quaternions
TFORM3  = '4E      '           / data format of field: 4-byte REAL
TTYPE4  = 'EIC     '           / Spacecraft position: Earth X, Y, & Z
TFORM4  = '3E      '           / data format of field: 4-byte REAL
TUNIT4  = 'km      '           / physical unit of field
TTYPE5  = 'TRIGRATE'           / Rates-14 detectors, 8 channels
TFORM5  = '112E    '           / data format of field: 4-byte REAL
TUNIT5  = 'count/s '           / physical unit of field
EXTNAME = 'TRIGRATE'           / name of this binary table extension
TDIM5   = '(14, 8) '           / Array dimensions of TRIGRATE data
TELESCOP= 'GLAST   '           / Name of mission/satellite
INSTRUME= 'GBM     '           / Specific instrument used for observation
OBSERVER= 'Meegan  '           / GLAST Burst Monitor P.I.
ORIGIN  = 'GIOC    '           / Name of organization making file
DATE    = '2023-08-17T07:42:39' / file creation date (YYYY-MM-DDThh:mm:ss UT)
DATE-OBS= '2023-08-17T07:32:41' / Date of start of observation
DATE-END= '2023-08-17T07:41:34' / Date of end of observation
TIMESYS = 'TT      '           / Time system used in time keywords
TIMEUNIT= 's       '           / Time since MJDREF, used in TSTART and TSTOP
MJDREFI =                51910 / MJD of GLAST reference epoch, integer part
MJDREFF = 7.428703703703703D-4 / MJD of GLAST reference epoch, fractional part
TSTART  =     713950361.515924 / [GLAST MET] Observation start time
TSTOP   =     713950894.003690 / [GLAST MET] Observation stop time
DETTYPE = 'BOTH    '           / Detector type: NAI or BGO
DATATYPE= 'TRIGDAT '           / Type of lookup table: CTIME or CSPEC
TRIGTIME=     713950412.140552 / Trigger time relative to MJDREF, double precisi
OBJECT  = 'UNRELOC230817315'   / Burst name in standard format, yymmddfff
RADECSYS= 'FK5     '           / Stellar reference frame
EQUINOX =               2000.0 / Equinox for RA and Dec
RA_OBJ  =             104.6667 / Calculated RA of burst
DEC_OBJ =              80.9333 / Calculated Dec of burst
ERR_RAD =              32.0667 / Calculated Location Error Radius
CHECKSUM= '9916A91349139913'   / HDU checksum updated 2023-08-17T07:42:39
DATASUM = '53829084'           / data unit checksum updated 2023-08-17T07:42:39

trigger/glg_trigdat_all_bn230817315_v00.fit: HDUList[2].header
XTENSION= 'BINTABLE'           / binary table extension
BITPIX  =                    8 / 8-bit bytes
NAXIS   =                    2 / 2-dimensional binary table
NAXIS1  =                  466 / width of table in bytes
NAXIS2  =                    1 / number of rows in table
PCOUNT  =                    0 / size of special data area
```

```
GCOUNT  =                    1 / one data group (required keyword)
TFIELDS =                    4 / number of fields in each row
TTYPE1  = 'TIME    '           / Start time of the background accumulation
TFORM1  = '1D      '           / data format of field: 8-byte DOUBLE
TUNIT1  = 's       '           / physical unit of field
TTYPE2  = 'ENDTIME '           / Creation time of the background model
TFORM2  = '1D      '           / data format of field: 8-byte DOUBLE
TUNIT2  = 's       '           / physical unit of field
TTYPE3  = 'QUALITY '           / Quality Flag for the background model
TFORM3  = '2B      '           / data format of field: BYTE
TTYPE4  = 'BCKRATES'           / Rates-14 detectors, 8 channels
TFORM4  = '112E    '           / data format of field: 4-byte REAL
TUNIT4  = 'count/s '           / physical unit of field
EXTNAME = 'BCKRATES'           / name of this binary table extension
TDIM4   = '(14, 8) '           / Array dimensions of BCKRATES data
TELESCOP= 'GLAST   '           / Name of mission/satellite
INSTRUME= 'GBM     '           / Specific instrument used for observation
DETNAM  = 'ALL     '           / Individual detector name
OBSERVER= 'Meegan  '           / GLAST Burst Monitor P.I.
ORIGIN  = 'GIOC    '           / Name of organization making file
DATE    = '2023-08-17T07:42:39' / file creation date (YYYY-MM-DDThh:mm:ss UT)
DATE-OBS= '2023-08-17T07:32:41' / Date of start of observation
DATE-END= '2023-08-17T07:41:34' / Date of end of observation
TIMESYS = 'TT      '           / Time system used in time keywords
TIMEUNIT= 's       '           / Time since MJDREF, used in TSTART and TSTOP
MJDREFI =                51910 / MJD of GLAST reference epoch, integer part
MJDREFF = 7.428703703703703D-4 / MJD of GLAST reference epoch, fractional part
TSTART  =     713950361.515924 / [GLAST MET] Observation start time
TSTOP   =     713950894.003690 / [GLAST MET] Observation stop time
DETTYPE = 'BOTH    '           / Detector type: NAI or BGO
DATATYPE= 'TRIGDAT '           / Type of lookup table: CTIME or CSPEC
TRIGTIME=     713950412.140552 / Trigger time relative to MJDREF, double precisi
OBJECT  = 'UNRELOC230817315'   / Burst name in standard format, yymmddfff
RADECSYS= 'FK5     '           / Stellar reference frame
EQUINOX =               2000.0 / Equinox for RA and Dec
RA_OBJ  =             104.6667 / Calculated RA of burst
DEC_OBJ =              80.9333 / Calculated Dec of burst
ERR_RAD =              32.0667 / Calculated Location Error Radius
CHECKSUM= 'Nn3dQm2ZNm2bNm2Z'   / HDU checksum updated 2023-08-17T07:42:39
DATASUM = '2673658102'         / data unit checksum updated 2023-08-17T07:42:39

trigger/glg_trigdat_all_bn230817315_v00.fit: HDUList[3].header
XTENSION= 'BINTABLE'           / binary table extension
BITPIX  =                    8 / 8-bit bytes
NAXIS   =                    2 / 2-dimensional binary table
NAXIS1  =                   86 / width of table in bytes
NAXIS2  =                    1 / number of rows in table
PCOUNT  =                    0 / size of special data area
GCOUNT  =                    1 / one data group (required keyword)
TFIELDS =                   15 / number of fields in each row
TTYPE1  = 'TIME    '           / End time of location rates accumulation
TFORM1  = '1D      '           / data format of field: 8-byte DOUBLE
TUNIT1  = 's       '           / physical unit of field
TTYPE2  = 'RA      '           / Calculated Right Ascension of source
TFORM2  = '1E      '           / data format of field: 4-byte REAL
```

```
TUNIT2  = 'deg     '           / physical unit of field
TTYPE3  = 'DEC     '           / Calculated Declination of source
TFORM3  = '1E      '           / data format of field: 4-byte REAL
TUNIT3  = 'deg     '           / physical unit of field
TTYPE4  = 'STATERR '           / Error radius of calculated location
TFORM4  = '1E      '           / data format of field: 4-byte REAL
TUNIT4  = 'deg     '           / physical unit of field
TTYPE5  = 'LOCALG  '           / Location algorithm used in calculation
TFORM5  = '1I      '           / data format of field: 2-byte INTEGER
TTYPE6  = 'EVTCLASS'           / Two highest probable event classes
TFORM6  = '2I      '           / data format of field: 2-byte INTEGER
TTYPE7  = 'RELIABLT'           / Reliabilities of probable event classes
TFORM7  = '2E      '           / data format of field: 4-byte REAL
TTYPE8  = 'INTNSITY'           / Standardized count intensity
TFORM8  = '1E      '           / data format of field: 4-byte REAL
TUNIT8  = 'count   '           / physical unit of field
TTYPE9  = 'HDRATIO '           / Standard hardness ratio (channels 3 / 4)
TFORM9  = '1E      '           / data format of field: 4-byte REAL
TTYPE10 = 'FLUENCE '           / Fluence counts in 3 + 4 energy band
TFORM10 = '1E      '           / data format of field: 4-byte REAL
TUNIT10 = 'count   '           / physical unit of field
TTYPE11 = 'SIGMA   '           / Significance of localization in sigma
TFORM11 = '1E      '           / data format of field: 4-byte REAL
TTYPE12 = 'LOCRATES'           / Localization rates-12 NaI detectors
TFORM12 = '12I     '           / data format of field: 2-byte INTEGER
TUNIT12 = 'count/s '           / physical unit of field
TTYPE13 = 'TRIG_TS '           / Location data timescale
TFORM13 = '1E      '           / data format of field: 4-byte REAL
TUNIT13 = 's       '           / physical unit of field
TTYPE14 = 'TR_SCAZ '           / Source azimuth with respect to Spacecraft
TFORM14 = '1E      '           / data format of field: 4-byte REAL
TUNIT14 = 'degree  '           / physical unit of field
TTYPE15 = 'TR_SCZEN'           / Source zenith with respect to Spacecraft
TFORM15 = '1E      '           / data format of field: 4-byte REAL
TUNIT15 = 'degree  '           / physical unit of field
EXTNAME = 'OB_CALC '           / name of this binary table extension
TELESCOP= 'GLAST   '           / Name of mission/satellite
INSTRUME= 'GBM     '           / Specific instrument used for observation
DETNAM  = 'ALL     '           / Individual detector name
OBSERVER= 'Meegan  '           / GLAST Burst Monitor P.I.
ORIGIN  = 'GIOC    '           / Name of organization making file
DATE    = '2023-08-17T07:42:39' / file creation date (YYYY-MM-DDThh:mm:ss UT)
DATE-OBS= '2023-08-17T07:32:41' / Date of start of observation
DATE-END= '2023-08-17T07:41:34' / Date of end of observation
TIMESYS = 'TT      '           / Time system used in time keywords
TIMEUNIT= 's       '           / Time since MJDREF, used in TSTART and TSTOP
MJDREFI =                51910 / MJD of GLAST reference epoch, integer part
MJDREFF = 7.428703703703703D-4 / MJD of GLAST reference epoch, fractional part
TSTART  =     713950361.515924 / [GLAST MET] Observation start time
TSTOP   =     713950894.003690 / [GLAST MET] Observation stop time
DETTYPE = 'BOTH    '           / Detector type: NAI or BGO
DATATYPE= 'TRIGDAT '           / Type of lookup table: CTIME or CSPEC
TRIGTIME=     713950412.140552 / Trigger time relative to MJDREF, double precisi
OBJECT  = 'UNRELOC230817315'   / Burst name in standard format, yymmddfff
RADECSYS= 'FK5     '           / Stellar reference frame
```

```
EQUINOX =               2000.0 / Equinox for RA and Dec
RA_OBJ  =             104.6667 / Calculated RA of burst
DEC_OBJ =              80.9333 / Calculated Dec of burst
ERR_RAD =              32.0667 / Calculated Location Error Radius
CHECKSUM= 'oTTAoQS9oQSAoQS9'   / HDU checksum updated 2023-08-17T07:42:39
DATASUM = '615958994'          / data unit checksum updated 2023-08-17T07:42:39

trigger/glg_trigdat_all_bn230817315_v00.fit: HDUList[4].header
XTENSION= 'BINTABLE'           / binary table extension
BITPIX  =                    8 / 8-bit bytes
NAXIS   =                    2 / 2-dimensional binary table
NAXIS1  =                  492 / width of table in bytes
NAXIS2  =                    1 / number of rows in table
PCOUNT  =                    0 / size of special data area
GCOUNT  =                    1 / one data group (required keyword)
TFIELDS =                    5 / number of fields in each row
TTYPE1  = 'TIME    '           / Beginning of accumulation, calculated value
TFORM1  = '1D      '           / data format of field: 8-byte DOUBLE
TUNIT1  = 's       '           / physical unit of field
TTYPE2  = 'ENDTIME '           / End of accumulation, same as PCKTTIME
TFORM2  = '1D      '           / data format of field: 8-byte DOUBLE
TUNIT2  = 's       '           / physical unit of field
TTYPE3  = 'SCATTITD'           / Spacecraft attitude quaternions
TFORM3  = '4E      '           / data format of field: 4-byte REAL
TTYPE4  = 'EIC     '           / Spacecraft position: Earth X, Y, & Z
TFORM4  = '3E      '           / data format of field: 4-byte REAL
TUNIT4  = 'km      '           / physical unit of field
TTYPE5  = 'MAXRATES'           / Rates-14 detectors, 8 channels
TFORM5  = '112E    '           / data format of field: 4-byte REAL
TUNIT5  = 'count/s '           / physical unit of field
EXTNAME = 'MAXRATES'           / name of this binary table extension
TDIM5   = '(14, 8) '           / Array dimensions of MAXRATES data
TELESCOP= 'GLAST   '           / Name of mission/satellite
INSTRUME= 'GBM     '           / Specific instrument used for observation
DETNAM  = 'ALL     '           / Individual detector name
OBSERVER= 'Meegan  '           / GLAST Burst Monitor P.I.
ORIGIN  = 'GIOC    '           / Name of organization making file
DATE    = '2023-08-17T07:42:39' / file creation date (YYYY-MM-DDThh:mm:ss UT)
DATE-OBS= '2023-08-17T07:32:41' / Date of start of observation
DATE-END= '2023-08-17T07:41:34' / Date of end of observation
TIMESYS = 'TT      '           / Time system used in time keywords
TIMEUNIT= 's       '           / Time since MJDREF, used in TSTART and TSTOP
MJDREFI =                51910 / MJD of GLAST reference epoch, integer part
MJDREFF = 7.428703703703703D-4 / MJD of GLAST reference epoch, fractional part
TSTART  =     713950361.515924 / [GLAST MET] Observation start time
TSTOP   =     713950894.003690 / [GLAST MET] Observation stop time
DETTYPE = 'BOTH    '           / Detector type: NAI or BGO
DATATYPE= 'TRIGDAT '           / Type of lookup table: CTIME or CSPEC
TRIGTIME=     713950412.140552 / Trigger time relative to MJDREF, double precisi
OBJECT  = 'UNRELOC230817315'   / Burst name in standard format, yymmddfff
RADECSYS= 'FK5     '           / Stellar reference frame
EQUINOX =               2000.0 / Equinox for RA and Dec
RA_OBJ  =             104.6667 / Calculated RA of burst
DEC_OBJ =              80.9333 / Calculated Dec of burst
ERR_RAD =              32.0667 / Calculated Location Error Radius
```

```
CHECKSUM= '9dLaCaIT9aIZCaIZ'   / HDU checksum updated 2023-08-17T07:42:39
DATASUM = '885688344'          / data unit checksum updated 2023-08-17T07:42:39

trigger/glg_trigdat_all_bn230817315_v00.fit: HDUList[5].header
XTENSION= 'BINTABLE'           / binary table extension
BITPIX  =                    8 / 8-bit bytes
NAXIS   =                    2 / 2-dimensional binary table
NAXIS1  =                  492 / width of table in bytes
NAXIS2  =                  153 / number of rows in table
PCOUNT  =                    0 / size of special data area
GCOUNT  =                    1 / one data group (required keyword)
TFIELDS =                    5 / number of fields in each row
TTYPE1  = 'TIME    '           / Beginning of accumulation, calculated value
TFORM1  = '1D      '           / data format of field: 8-byte DOUBLE
TUNIT1  = 's       '           / physical unit of field
TTYPE2  = 'ENDTIME '           / End of accumulation, same as PCKTTIME
TFORM2  = '1D      '           / data format of field: 8-byte DOUBLE
TUNIT2  = 's       '           / physical unit of field
TTYPE3  = 'SCATTITD'           / Spacecraft attitude quaternions
TFORM3  = '4E      '           / data format of field: 4-byte REAL
TTYPE4  = 'EIC     '           / Spacecraft position: Earth X, Y, & Z
TFORM4  = '3E      '           / data format of field: 4-byte REAL
TUNIT4  = 'km      '           / physical unit of field
TTYPE5  = 'RATE    '           / Rates-14 detectors, 8 channels
TFORM5  = '112E    '           / data format of field: 4-byte REAL
TUNIT5  = 'count/s '           / physical unit of field
EXTNAME = 'EVNTRATE'           / name of this binary table extension
TDIM5   = '(14, 8) '           / Array dimensions of EVNTRATE data
TELESCOP= 'GLAST   '           / Name of mission/satellite
INSTRUME= 'GBM     '           / Specific instrument used for observation
DETNAM  = 'ALL     '           / Individual detector name
OBSERVER= 'Meegan  '           / GLAST Burst Monitor P.I.
ORIGIN  = 'GIOC    '           / Name of organization making file
DATE    = '2023-08-17T07:42:39' / file creation date (YYYY-MM-DDThh:mm:ss UT)
DATE-OBS= '2023-08-17T07:32:41' / Date of start of observation
DATE-END= '2023-08-17T07:41:34' / Date of end of observation
TIMESYS = 'TT      '           / Time system used in time keywords
TIMEUNIT= 's       '           / Time since MJDREF, used in TSTART and TSTOP
MJDREFI =                51910 / MJD of GLAST reference epoch, integer part
MJDREFF = 7.428703703703703D-4 / MJD of GLAST reference epoch, fractional part
TSTART  =     713950361.515924 / [GLAST MET] Observation start time
TSTOP   =     713950894.003690 / [GLAST MET] Observation stop time
DETTYPE = 'BOTH    '           / Detector type: NAI or BGO
DATATYPE= 'TRIGDAT '           / Type of lookup table: CTIME or CSPEC
TRIGTIME=     713950412.140552 / Trigger time relative to MJDREF, double precisi
OBJECT  = 'UNRELOC230817315'   / Burst name in standard format, yymmddfff
RADECSYS= 'FK5     '           / Stellar reference frame
EQUINOX =               2000.0 / Equinox for RA and Dec
RA_OBJ  =             104.6667 / Calculated RA of burst
DEC_OBJ =              80.9333 / Calculated Dec of burst
ERR_RAD =              32.0667 / Calculated Location Error Radius
CHECKSUM= 'JiXWKZWWJfWWJZWW'   / HDU checksum updated 2023-08-17T07:42:39
DATASUM = '1654709740'         / data unit checksum updated 2023-08-17T07:42:39
```

```
burst/glg_healpix_all_bn230101095.fit: HDUList[0].header
SIMPLE  =                    T / conforms to FITS standard
BITPIX  =                    8 / array data type
NAXIS   =                    0 / number of array dimensions
EXTEND  =                    T
CREATOR = 'GBM_healpix.py 2.0'
FILETYPE= 'IMAGE   '           / Name for this type of FITS file
TELESCOP= 'GLAST   '           / Name of mission/satellite
INSTRUME= 'GBM     '           / Specific instrument used for observation
OBSERVER= 'Meegan  '           / GLAST Burst Monitor P.I.
ORIGIN  = 'GIOC    '           / Name of organization making file
DATE    = '2023-01-01T02:26:37' / file creation date (YYYY-MM-DDThh:mm:ss UT)
DATE-OBS= '2023-01-01T02:14:27' / Date of start of observation
DATE-END= '2023-01-01T02:24:41' / Date of end of observation
TIMESYS = 'TT      '           / Time system used in time keywords
TIMEUNIT= 's       '           / Time since MJDREF, used in TSTART and TSTOP
MJDREFI =                51910 / MJD of GLAST reference epoch, integer part
MJDREFF = '7.428703703703703e-4' / MJD of GLAST reference epoch, fractional part
TSTART  =     694232067.035982 / [GLAST MET] Observation start time
TSTOP   =     694232681.448828 / [GLAST MET] Observation stop time
FILENAME= 'glg_healpix_all_bn230101095_v00.fit' / Name of this file
TRIGTIME=     694232203.998664 / Trigger time relative to MJDREF, double precisi
OBJECT  = 'GRB230101095'       / Burst name in standard format, yymmddfff
RADECSYS= 'FK5     '           / Stellar reference frame
EQUINOX =               2000.0 / Equinox for RA and Dec
RA_OBJ  =                206.3 / Calculated RA of burst
DEC_OBJ =               -21.94 / Calculated Dec of burst
ERR_RAD =                 2.79 / Calculated Location Error Radius
THETA   =                 49.0 / [deg] Angle from spacecraft zenith
PHI     =                282.0 / [deg] Angle from spacecraft +X axis toward +Y
LOC_SRC = 'Fermi, GBM'         / Mission/Instrument providing the localization
CLASS   = 'GRB     '           / Classification of trigger
OBJ_CLAS= 'GRB     '           / Classification of trigger
GEO_LONG=             105.3333 / [deg] Spacecraft geographical east longitude
GEO_LAT =   -8.583299999999999 / [deg] Spacecraft geographical north latitude
RA_SCX  =             300.1503 / [deg] Pointing of spacecraft x-axis: RA
DEC_SCX =             -33.2745 / [deg] Pointing of spacecraft x-axis: Dec
RA_SCZ  =             225.9636 / [deg] Pointing of spacecraft z-axis: RA
DEC_SCZ =              22.5506 / [deg] Pointing of spacecraft z-axis: Dec
LOC_VER = '3       '           / Version string of localizing software
LOC_ENRG= '(50, 300)'          / Energy range used for localization
LMETHOD = 'Interactive'        / Method of localization
CHECKSUM= 'iQ8Ji07Ii07Ii07I'   / HDU checksum updated 2023-01-01T02:26:38
DATASUM = '0       '           / data unit checksum updated 2023-01-01T02:26:38

burst/glg_healpix_all_bn230101095.fit: HDUList[1].header
XTENSION= 'BINTABLE'           / binary table extension
BITPIX  =                    8 / array data type
NAXIS   =                    2 / number of array dimensions
NAXIS1  =                 8192 / length of dimension 1
NAXIS2  =                  192 / length of dimension 2
PCOUNT  =                    0 / number of group parameters
GCOUNT  =                    1 / number of groups
TFIELDS =                    2 / number of table fields
TTYPE1  = 'PROBABILITY'        / Differential probability per pixel
```

```
TFORM1  = '1024E   '
TTYPE2  = 'SIGNIFICANCE'       / Integrated probability
TFORM2  = '1024E   '
PIXTYPE = 'HEALPIX '           / HEALPIX pixelisation
ORDERING= 'NESTED  '           / Pixel ordering scheme, either RING or NESTED
COORDSYS= 'C       '           / Ecliptic, Galactic or Celestial (equatorial)
EXTNAME = 'HEALPIX '           / name of this binary table extension
NSIDE   =                  128 / Resolution parameter of HEALPIX
FIRSTPIX=                    0 / First pixel # (0 based)
LASTPIX =               196608 / Last pixel # (0 based)
INDXSCHM= 'IMPLICIT'           / Indexing: IMPLICIT or EXPLICIT
OBJECT  = 'GRB230101095'       / Sky coverage, either FULLSKY or PARTIAL
SUN_RA  =    280.9459905306383 / RA of Sun
SUN_DEC =   -23.05491259650264 / Dec of Sun
GEO_RA  =    60.47929839804375 / RA of Geocenter relative to Fermi
GEO_DEC =    8.384612241230409 / Dec of Geocenter relative to Fermi
GEO_RAD =    67.60608877134906 / Radius of the Earth
N0_RA   =    248.6679650941325 / RA pointing for detector n0
N0_DEC  =     24.7270202419298 / Dec pointing for detector n0
N1_RA   =    275.4366707619914 / RA pointing for detector n1
N1_DEC  =    21.76810402882301 / Dec pointing for detector n1
N2_RA   =    325.2747679543477 / RA pointing for detector n2
N2_DEC  =    19.80604679136331 / Dec pointing for detector n2
N3_RA   =    232.4182975656652 / RA pointing for detector n3
N3_DEC  =   -21.76481216175521 / Dec pointing for detector n3
N4_RA   =    217.0254332698711 / RA pointing for detector n4
N4_DEC  =    -66.9365511563602 / Dec pointing for detector n4
N5_RA   =    301.5114572426571 / RA pointing for detector n5
N5_DEC  =   -30.31816048405326 / Dec pointing for detector n5
N6_RA   =    204.8074775477132 / RA pointing for detector n6
N6_DEC  =    18.74795286238482 / Dec pointing for detector n6
N7_RA   =    179.6047473474741 / RA pointing for detector n7
N7_DEC  =    10.38278821502396 / Dec pointing for detector n7
N8_RA   =    144.2978879941191 / RA pointing for detector n8
N8_DEC  =   -18.21597523412012 / Dec pointing for detector n8
N9_RA   =    210.2684229583013 / RA pointing for detector n9
N9_DEC  =    67.52339112892444 / Dec pointing for detector n9
NA_RA   =    38.70694341423297 / RA pointing for detector na
NA_DEC  =    66.33006706865352 / Dec pointing for detector na
NB_RA   =    121.6037164770696 / RA pointing for detector nb
NB_DEC  =    29.92088435571887 / Dec pointing for detector nb
B0_RA   =    299.9059847374708 / RA pointing for detector b0
B0_DEC  =   -33.38537832393065 / Dec pointing for detector b0
B1_RA   =    119.9059847374708 / RA pointing for detector b1
B1_DEC  =    33.38537832393065 / Dec pointing for detector b1
CHECKSUM= '7ce29ad07ad07ad0'   / HDU checksum updated 2023-01-01T02:26:38
DATASUM = '2195425426'         / data unit checksum updated 2023-01-01T02:26:38
COMMENT SCPOS: [-3362250. -5937750. -1005750.]
COMMENT QUAT: [ 0.550389  -0.0339537 -0.53916    0.636573 ]
```